

Observed decreases in on-road CO₂ concentrations in Beijing during COVID-19 restrictions

Di Liu¹, Wanqi Sun², Ning Zeng^{3,4}, Pengfei Han^{1*}, Bo Yao^{2,*}, Zhiqiang Liu¹, Pucai Wang⁵, Ke Zheng¹, Han Mei¹, Qixiang Cai¹

¹Laboratory of Numerical Modeling for Atmospheric Sciences & Geophysical Fluid Dynamics, Institute of Atmospheric Physics, Chinese Academy of Sciences

²Meteorological Observation Centre, China Meteorological Administration, Beijing, China

³Department of Atmospheric and Oceanic Science, University of Maryland, USA

⁴Earth System Science Interdisciplinary Center, University of Maryland, USA

⁵Laboratory for Middle Atmosphere and Global Environment Observation, Institute of Atmospheric Physics, Chinese Academy of Sciences

* Correspondence to: Pengfei Han (pphan@mail.iap.ac.cn); Bo Yao (yaob@cma.gov.cn)

Abstract:

To prevent the spread of the COVID-19 epidemic, restrictions such as “lockdowns”, were conducted globally, which led to a significant reduction in fossil fuel emissions, especially in urban ~~regions~~ areas. However, CO₂ concentrations in urban ~~regions~~ areas are affected by many factors, such as weather, ~~biological sinks~~ and background CO₂ fluctuations. Thus, it is difficult to directly observe the ~~CO₂ reductions~~ in CO₂ concentrations with from sparse ground observations. Here, we focus on urban ground transportation emissions, which were dramatically affected by the ~~prohibitions~~ restrictions, to determine the reduction signals. We conducted six ~~series of~~ on-road CO₂ observations in Beijing using mobile platforms before (BC), during (DC) and after ~~COVID-19 prohibitions~~ (AC) ~~the implementation of COVID-19 restrictions~~. To reduce ~~the impacts of~~ the weather ~~conditions~~ and background ~~impacts~~ fluctuations, we ~~analyze vehicle~~ trips with the most similar weather ~~condition~~ as possible and calculated the enhancement ~~metric~~, which ~~is mean~~ the difference ~~in the CO₂ concentration~~ between the on-road ~~CO₂ concentration~~ and the “urban background” ~~CO₂ concentration level~~ measured at the ~~tower of the~~ Institute of Atmospheric Physics (IAP), Chinese Academy of Sciences (~~IAP~~ tower). The results showed that ~~the~~ DC CO₂ enhancement ~~was~~ decreased by 41 (± 1.3) parts per million (ppm) and 26 (± 6.2) ppm compared to those ~~for the~~ ~~during~~ BC and AC ~~trips~~, respectively, ~~after eliminating the fluctuations in CO₂ concentrations on polluted days~~. Detailed analysis showed that, during ~~COVID-19 restrictions~~, there was no difference between weekdays and weekends ~~during working hours (9:00-17:00 local standard time, LST)~~. The enhancements during rush hours (7:00-9:00 and 17:00-20:00 LST) were almost twice those during working hours, indicating that emissions during rush hours were much higher. ~~Compared For with~~ DC and BC, the ~~reductions in the~~ enhancements ~~reductions~~ during rush hours were much larger than those during working hours. Our findings showed a clear ~~CO₂ concentration~~ decrease during ~~COVID-19 restrictions~~, which ~~are is~~ consistent with the CO₂ ~~concentration and~~ emissions reductions due to the pandemic. The enhancement ~~way~~ method used in this study is an effective method to reduce the impacts of weather and background fluctuations, ~~and~~ low-cost sensors, which are inexpensive and convenient, could play an important role in further on-road and other urban observations ~~should be regularly and more frequently conducted in future work~~.

带格式的: 字体: (默认) 宋体, (中文) 宋体, 小四

带格式的: 正文, 段落间距段前: 0磅, 段后: 0磅

带格式的: 下标

带格式的: 下标

Introduction:

Since December 2019, the world has been fiercely struggling against a pandemic of a novel ~~c~~Coronavirus named COVID-19, which was ~~firstly-first~~ identified in Wuhan, China (Gross et al., 2020); and then quickly identified ~~by-in~~ other countries ~~in-of~~ East Asia, ~~and~~ Europe and the United States ~~according to World Health Organization Novel Coronavirus (2019-nCoV) situation reports~~ (https://www.who.int/emergencies/diseases/novel-coronavirus-2019/situation-reports(Le Quere et al., 2020)). In Beijing, the first case was confirmed on 20th January 2020, ~~and~~ followed by a quick increase in confirmed cases (SFigure 1A). From 24th January to 30th April, Beijing enacted a Level-1 response to major public health emergencies (red region, ~~in~~ SFigure 1), and lowered the response to Level-2 from 30th April to 6th June, after “zero growth” persisted for almost one month (yellow region, ~~in~~ SFigure 1).

As the world faced this highly infectious pandemic without efficient medication, governments ~~enacted-out~~ similar ~~prohibitions-restrictions~~ to prevent the spread of the virus: isolating cases, enacting stay-~~at-~~home orders, forbidding mass gatherings, and closing factories and schools. These ~~prohibitions-restrictions~~ highly altered the ~~industrial factory~~ production, energy consumption and transportation volume and led to sharp emissions reductions (Liu et al., 2020; Le Quere et al., 2020). As previous inventory studies estimated, ~~by early April 2020~~, the global daily CO₂ emissions ~~had~~ decreased by 17% (11 to 25% for $\pm 1\sigma$) ~~by early April 2020~~ compared with ~~those in the mean~~ 2019 levels, and the ~~absolute-total~~ reduction was approximately 1048 (543 to 1,638) MtCO₂ ~~until-at~~ the end of April (Le Quere et al., 2020). ~~Among these emissions,~~ ~~e~~Emissions from ground transportation obviously decreased by 36% ~~(28 to 46)~~ (Le Quere et al., 2020). According to Liu et al. (Liu et al., 2020), emissions ~~decreases~~ in China ~~decreased were~~ 6.97% from January to April 2020, ~~in-with which~~ ground transportation emissions dropp~~ing~~ed abruptly by 53.4% in February and continu~~ing~~ed to decrease by 25.96% in March (SFigure 1B and 1C). In Beijing, during the first quarter ~~in-of~~ 2020, passenger traffic volumes decreased 55.66%, and ground transport volumes decreased 35.2% according to the distance-weighted passenger and freight turnover (Han et al., 2020).

~~Although~~ ~~u~~Urban areas are the main CO₂ sources and account for more than 70% of fossil fuel emissions (Rosenzweig et al., 2010), ~~and the~~ CO₂ concentrations in urban areas ~~is-are~~ dominated by weather changes (Woodwell et al., 1973; Grimmond et al., 2002); ~~for example, high wind speed accelerates the mixing and diffusion of CO₂~~. In addition, the ~~absolute~~ carbon emission reductions (258 MtC, from Le Quere et al. (Le Quere et al., 2020)) due to COVID-19 ~~restrictions~~ ~~was-were~~ relatively small compared to the CO₂ content in the atmosphere (860 GtC, from Friedlingstein et al. (Friedlingstein et al., 2019)) ~~and-~~ carbon uptake by vegetation (the average seasonal amplitude of the net land-atmosphere carbon flux is 41.6 GtC/yr, from Zeng et al. (Zeng et al., 2014)). Therefore, it is ~~very~~ difficult to detect ~~CO₂ concentration~~ decreases in the urban ~~areas~~ ~~CO₂ concentration decrease~~ directly ~~by-from~~ sparse ground observations (Kutsch et al., 2020; Ott et al., 2020). For example, according to the daily CO₂ concentrations in 2019 and 2020 recorded by the ~~tower at the~~ Institute of Atmospheric Physics (IAP), Chinese Academy of Sciences (~~IAP~~) ~~tower~~, even though Beijing was within the strictest control/confinement period from 10th to 14th February 2020, stable weather (~~in which the planetary boundary layer heights (PBLHs) were only ~600 m~~ ~~poor diffusion conditions~~) led to CO₂ concentrations that were approximately 90 parts per million (ppm) higher than those on the same date in 2019 (~~PBLHs were ~ 900 m~~) (SFigure 1D). Sussmann and Rettinger (2020) also proved it. ~~Although-Despite~~ global emissions reductions due to COVID-19 ~~restrictions~~, they found a historic record high in column-averaged atmospheric carbon dioxide (XCO₂) in April 2020 by using Total Carbon Column Observation Network (TCCON) data. ~~By a~~ Assuming ~~that the a~~ COVID-19-related CO₂ growth rate reduction of 0.32 ppm/yr² in 2020 ~~for-at~~ Mauna Loa ~~to-be~~ true and measured (from ~~the~~ UK Met Office; ~~an-~~ overall 8% emissions reductions in 2020), they found ~~that~~ there is ~~a~~ ~0.6 year ‘delay’ to separate TCCON-measured growth rates and the reference forecast (~~without absence of~~ COVID-19 ~~restrictions~~).

域代码已更改

域代码已更改

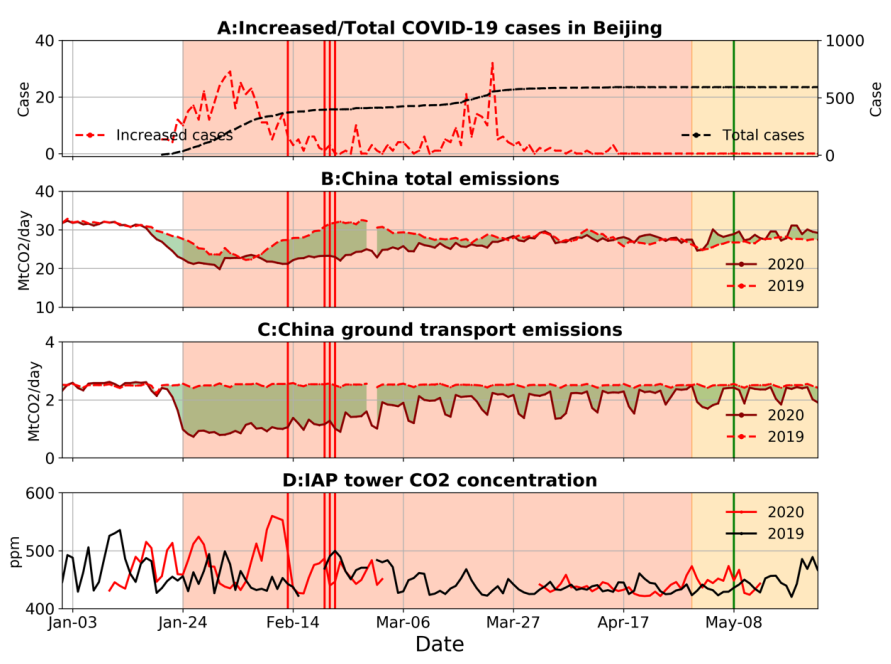
带格式的: 字体: (默认) Times
New Roman, 10 磅

85 With the knowledge that urban ground transportation was strongly suppressed due to COVID-19 restrictions, we designed on-road observations by using a mobile platform to find-detect reduction signals. These observations based on mobile platforms, which could provide CO₂ data with higher spatiotemporal resolution CO₂ data than satellite and ground observations, and have been widely conducted-used for carbon monitoring in urban and sub-urban regions-areas (for instance, on-road CO₂ concentration distributions were presented as transects in urban areas along routes-transects-of communities) (Idso et al., 2001; Bush et al., 2015; Sun et al., 2019). Almost However, all-all studies explained-agreed that weather (for example, wind speed, which is directly associated with the diffusion condition CO₂ mixing and dilution) is a dominant factor and should be considered during analysis. Reducing the impact of weather- However, it is still a problem at-to reduce the impact of weather. On the other hand, examining the enhancement, which is the calculate-ds the difference in the CO₂ concentration between urban and rural background observations, could effectively reduce the influence of background CO₂ concentration-fluctuations, to-analyze CO₂ concentration characteristics in urban areas and this metric has been widely used for monitoring urban carbon emissions and CO₂ concentrations (Idso et al., 1998; Idso et al., 2002; George et al., 2007; Mitchell et al., 2018; Perez et al., 2009).

带格式的：下标

带格式的：下标

100 To determine the CO₂ concentration reduction “signal” due to decreased ground transportation emissions decrease during COVID-19 restrictions, we first chose the most similar weather conditions as possible; second, and we calculated the enhancements metric by using subtracting the “baseline” IAP tower CO₂ concentration from the observed on-road CO₂ observations-concentration minus the “baseline” IAP tower CO₂ concentration to reduce impact of the influence from the background CO₂ fluctuations-in the background CO₂ concentration due to weather. Our results may provide direct evidence of ground transportation emission reductions due to COVID-19 restrictions, and this method could be an appropriate tool to analyze the CO₂ concentration and emissions related to of urban ground transportation in the future works.



110 *Figure 1. (A) Confirmed increased cases (red) and total cases (black) of COVID-19 in Beijing in 2020; the red/yellow region is the Level 1/2 response periods; vertical lines indicate the on roads observation dates, red/green lines indicate during and after COVID, respectively. One trip was conducted on 20th February 2019, which was not plotted in Figure 1. (B) China*

daily CO₂ emissions in the five months of 2019 (dotted line) and 2020 (solid line), data from Liu et al. (Liu et al., 2020). (C) China ground transport daily CO₂ emissions in the first five months of 2019 and 2020, data from Liu et al. (Liu et al., 2020). (D) Comparison of IAP tower CO₂ concentrations in 2019 (black) and 2020 (red).

115 Methods and Data:

We conducted six on-road observations in Beijing using mobile platforms before (BC; 1 trip: 20th February 2019), during (DC; 4 trips: 13th, 20th, 21st and 22nd February 2020) and after (AC; 1 trip: 9th May 2020) COVID-19 restrictions control (vertical lines in SFigure 1 indicate the trip dates). These trips covered the four ring roads that circled the city; which are the 2nd (with length of 332.7 km), 3rd (48 km), 4th (64 km) and 5th (99 km) rRing rRoads, from innermost to outermost, as shown in Figure 12. All trips were conducted during the daytime; in which four of them were on weekdays and two others were on a Saturday. Four trips covered at least one rush hour (7:00-9:00 local standard time (LST) for morning rush hour; 17:00-20:00 LST for evening).

To reduce the influence of the background CO₂ fluctuations, we first chose the similar weather conditions. As shown in Table 1, Three-four elements-aspects were considered: (1) real-time panoramic reality-photographs collected from the IAP tower (photograph available from: <http://view.iap.ac.cn:8080/imageview/>); (2) the PM_{2.5} (atmospheric particulate matter that has with a diameter of less than 2.5 μm) concentration from the Olympic Sports Center Station (40.003 °N, 116.407 °E, 5 m height, purple square in Figure 12A), which is run by the Ministry of Ecology and Environment of China (Zhang et al., 2015); (3) and wind speed data (available collected from: <https://www.wunderground.com/history/daily/cn/beijing/ZBNY/date/2020-5-9>); and (4) PBLH data, which are related to vertical mixing and diffusion of pollution/CO₂ emitted near the ground (Su et al., 2018). These data were collected from National Centers for Environmental Prediction Global Forecast System (GFS) reanalysis dataset (resolution: 0.25° × 0.25°), which is a globally gridded dataset representing the state of the Earth's atmosphere and incorporating observations and numerical weather prediction model output.

Then, on-road CO₂ concentration enhancements were calculated by subtracting the simultaneous CO₂ concentrations from detected at the IAP tower, which served as implies the “baseline” in for Beijing city (Eq. 1).

$$\text{CO}_2 \text{ enhancement} = \text{CO}_2 \text{ (on-road)} - \text{CO}_2 \text{ (IAP tower)} \quad (\text{Eq. 1})$$

带格式的：非上标/下标

带格式的：下标

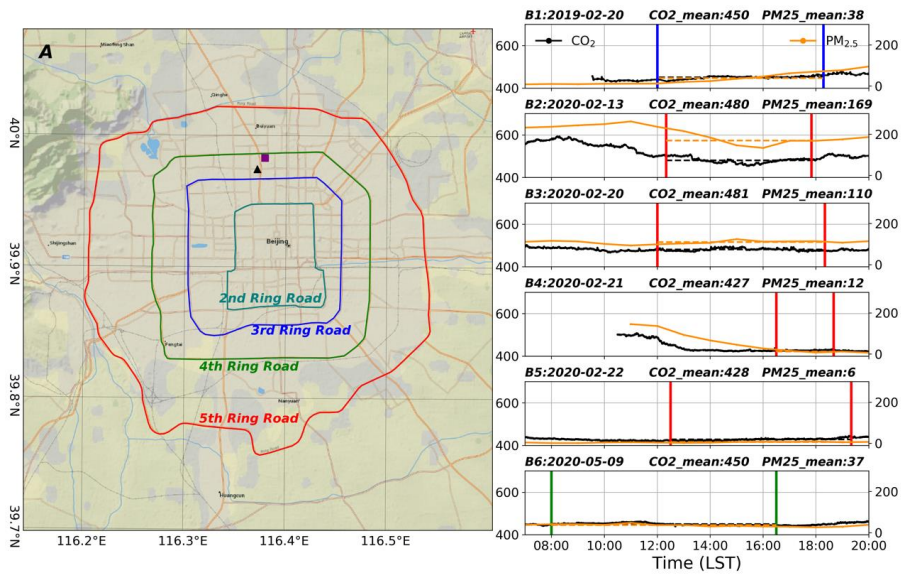


Figure 12. A: The locations of the 2nd, 3rd, 4th and 5th Ring Roads, the IAP tower (black triangle) and Olympic Sports Centre station (purple square); B1-B6: CO₂ concentration from at the IAP tower and PM_{2.5} concentration data from the Olympic Sports Center station during six trips.

145

Table 1. Weather conditions during six trips.


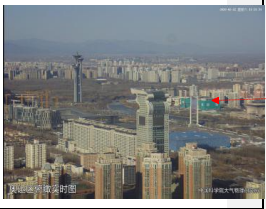

Label/date	Weather condition	Air condition (PM2.5: $\mu\text{g}/\text{m}^3$)	Wind speed (m/s)	PBLH (m)	Real-time panoramic photographs Reality photos
BC 2019-2-20 (Wed)	Clear day	38	2.5	897.7	
DC 2020-2-13 (Fri)	Light-Heavily polluted day	169	2.5	589	
DC 2020-2-20 (Fri)	Lightly-polluted day	110	1.3	691	

带格式表格

带格式的：居中

带格式的：居中

带格式的：居中

DC 2020-2-21 (Fri)	Clear day	12	2.5	<u>1587</u>	
DC 2020-2-22 (Fri)	Clear day	6	3.6	<u>1113</u>	
AC 2020-5-9 (Sat)	Clear day	37	1.6	<u>608</u>	

带格式的：居中

带格式的：居中

带格式的：居中

IAP tower CO₂ concentration at IAP tower data:

The IAP tower is a 325 m-high meteorological tower located at 116.3667 E, 39.9667 N, 49 m above sea level in northwest Beijing (Figure 12, black triangle) (Cheng et al., 2018). There are three levels of CO₂ concentration was determined at three levels records in this study: surface level (~2 m above the ground), lower level (~80 m) and upper level (~280 m) (Cheng et al., 2018). The CO₂ concentrations were measured by a Picarro G2301 greenhouse gas concentration analyzer (Picarro, 2019). The instrument is was calibrated by using standard gas for every 3 hours, and each calibration lasted 5 minutes by using standard gas. The standard gasses were from the Meteorological Observation Center of the China Meteorological Administration (MOC/CMA) and, which were traced to the World Meteorological Organization (WMO) X2007 scale, and each calibration lasts for 5 minutes. The measurement precision-accuracy is was ~0.1 ppm. All The CO₂ concentrations were was recorded by every 2 seconds, and these data were then averaged into 1-minute intervals. Before 2020 (including the trip on 20th February 2019), the CO₂ concentrations were was measured at the lower and upper levels alternately for every 5 minutes, and the measurement at each level lasted 5 minutes. After 2020 (including the other 5 trips), the CO₂ concentration was continuously measured at the surface level. To maintain consistency as much as possible, we used the lower level/lower-level CO₂ concentrations before 2020 and the surface levels CO₂ after 2020.

带格式的：左

带格式的：下标

On-road CO₂ concentration data:

Three different CO₂-observation instruments were carried by vehicles for during six on-road trips (Table 2).

- 1) On 20th February 2019, a Picarro G2401 (Picarro, 2017) was adopted and installed on a vehicle; the air intake was set on the roof of the vehicle to avoid potential contact with direct plumes emitted from surrounding cars. The intake was linked/connected through a 2 m pipe with a particulate matter filter to the Picarro system (Figure 23A and 23B). The instruments characteristics and precision-accuracy have been described by Sun et al. (Sun et al., 2019). The CO₂ concentrations were collected every 2 seconds and then averaged into 1-minute intervals.
- 2) During COVID-19 restrictions (surveys on 13th, 20th, 21st and 22nd February 2020), a LI-COR LI-7810 CH₄/CO₂/H₂O trace gas analyzer was adopted, which uses optical feedback-cavity enhanced absorption spectroscopy technology (LI-COR, 2019). This instrument could obtain a CO₂ concentration with a precision-precision of 3.5 ppm for 1 second and within 1 ppm after 1-minute averaging (laboratory testing). The observation platform of the LI-7810 was

similar to that of the Picarro system. Before departure, the instrument was calibrated by using standard calibration gas ~~(from MOC/CMA)~~ to correct the drift.

- 3) On 9th May 2020, a low-cost light sensor was adopted and installed on the front windshield of the vehicle (Figure 23C). The instrument mainly consisted of three non-dispersive infrared (NDIR) CO₂ measurement sensors (named K30), and one environment (temperature, humidity and pressure) sensor (named BME). Although the original precision of each K30 ~~is-was~~ ± 30 ppm, after calibration and environmental correction in the laboratory and before departure, ~~the accuracy~~ was improved to within ± 5 ppm comparing with Picarro (Martin et al., 2017; SenseAir, 2019). Here, we used three K30s in one instrument to recognize and eliminate data anomalies and used the averaged CO₂ concentrations from the three K30s for analysis. Figure 34 shows the details of the experiment conducted on 22nd February 2020, for which ~~installed~~ one low-cost light sensor and Picarro were installed on the same vehicle for on-road monitoring. The results showed that the low-cost light sensor results ~~are-were~~ highly consistent with those of the Picarro system, with root mean square errors (RMSEs) less than 5 ppm.

Table 2. Instrument parameters ~~of for~~ six on-road observations

Label	Date	Instrument	Precision Accuracy	Temporal resolution (original->processed)
BC	2019-2-20	Picarro G2401	± 0.1 ppm	2 seconds -> 1 minute
DC	2020-2-13	LI-COR LI-7810	± 3.5 ppm (for 1 second); improved into ± 1 ppm (for 1 minute)	1 second -> 1 minute
	2020-2-20	LI-COR LI-7810		
	2020-2-21	LI-COR LI-7810		
	2020-2-22	LI-COR LI-7810		
AC	2020-5-9	Low-cost Sensor (K30)	± 5 ppm	2 seconds -> 1 minute

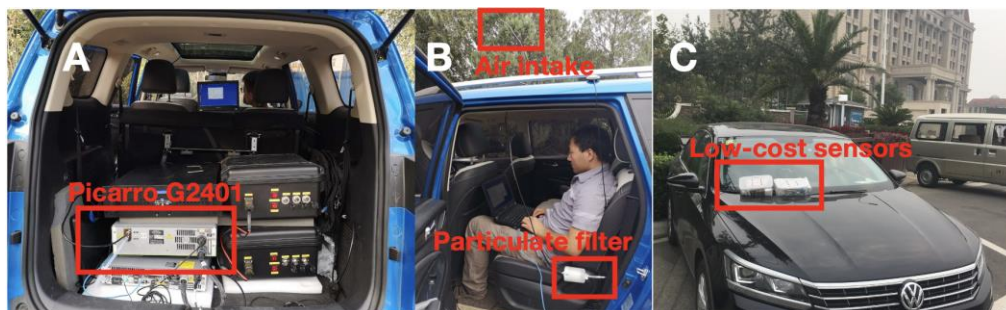
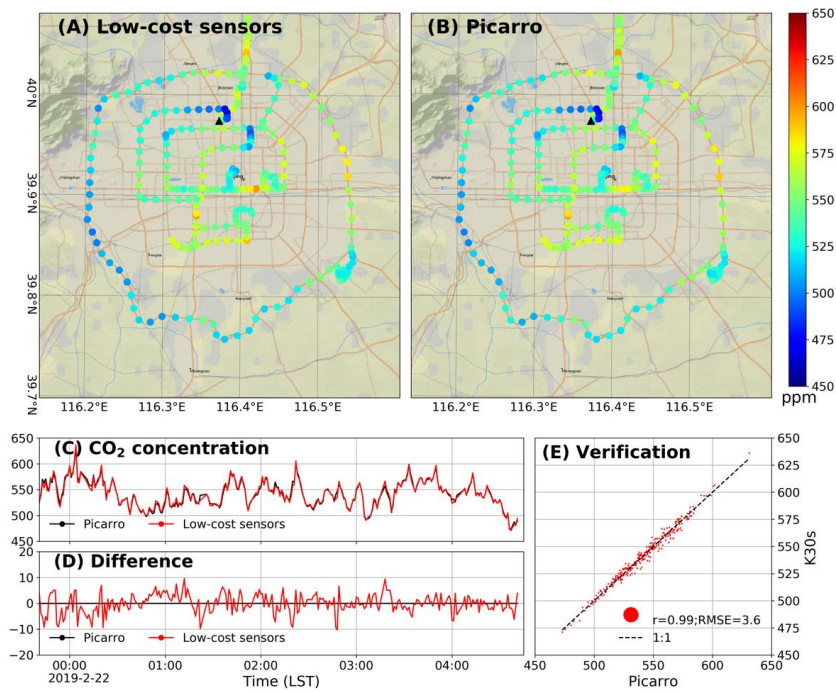
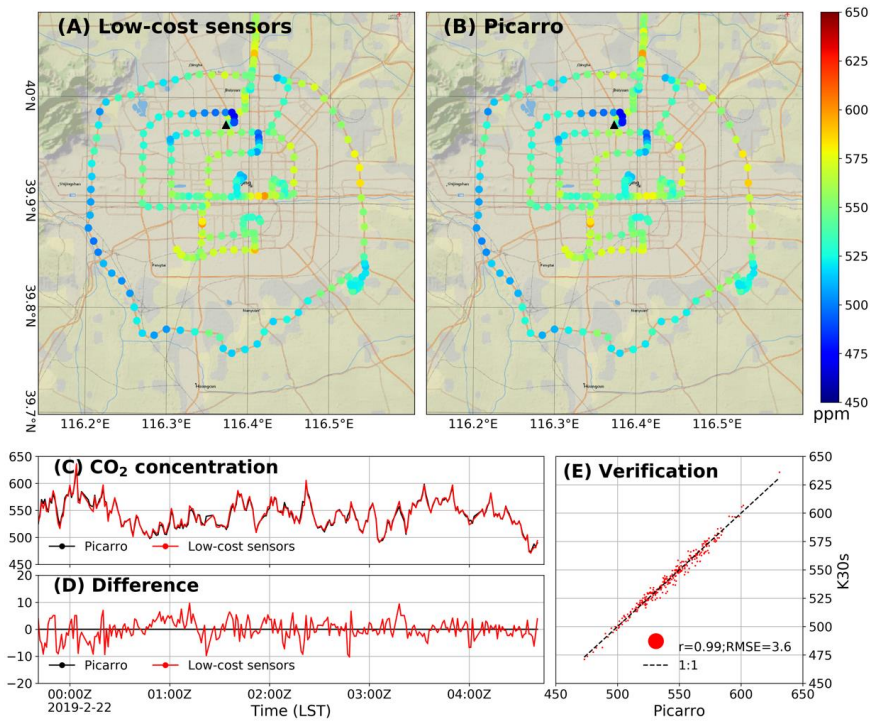


Figure 23. Photographs of the instrument installation for the during on-road observations. (A) and (B) Picarro system installed in the vehicle; (C) low-cost non-dispersive infrared (NDIR) sensors installed on the front windshield of the vehicle.



195 Figure 3.4. Verification of low-cost sensors for on-road observations. (A): ~~Map of CO₂ concentrations measured by~~ ~~map of~~
the low-cost sensor; (B): ~~map of the CO₂ concentration~~ ~~of measured by the~~ Picarro ~~system~~ on the same vehicle; (C): time
series of ~~the CO₂ concentrations measured by the~~ ~~using the~~ low-cost sensor and Picarro ~~system~~;
200 (D): difference (low-cost sensor ~~concentration~~ minus Picarro ~~concentration~~); (E): scatter plot of the low-cost sensor and Picarro ~~data~~, with an RMSE
of 3.6 ppm.

Auxiliary data and analysis:

The global positioning system (GPS) data ~~during for~~ BC and DC were collected by a GPS receiver (BS-70DU) (Sun et al.,
2019). ~~During For~~ AC, the data were collected by using mobile software (GPS Tracks), which provided time, longitude,
205 latitude, speed and altitude at 1-second resolution. These geographic information data were averaged into 1-minute intervals
and then matched with ~~the~~ CO₂ concentration data according to time.

Two remote sensing images were adopted (captured on 21st February 2019 at 11:40:00 ~~Local Standard Time (LST)~~, from a
Google Earth image, with 0.37 m spatial resolution; 19th February 2020 at 10:20:08 LST, from a Beijing-2 remote sensing
210 satellites panchromatic image, with 0.8 m spatial resolution). Considering the availability of data, we used the images from
the closest date and only part of the urban area. The comparison region covered ~~103.4~~ km of the ~~4th-3rd~~ Ring Road
(accounting for ~~20.51~~ % of the whole road, ~~for which the total length is 65.3 km~~) and ~~13.40~~ km of the ~~3rd-4th~~ Ring Road (~~also~~
~~accounting for 210.7~~ % of the whole road, ~~for which the length is 48.3 km~~). We used a visual interpretation method to obtain
the numbers of vehicles on the ~~3rd and 4th and 3rd~~ Ring Roads ~~for BC and DC before and during the COVID-19~~, respectively.

带格式的: 上标

215 ~~To understand the traffic situation, we also collected the real-time traffic congestion conditions (for each road), road name,~~
~~geographic information, road type and average speed as one-hour data from the Autonavi Open Platform~~
~~(<https://lbs.amap.com/>).~~

Results:

220 **On-road CO₂ concentration:**

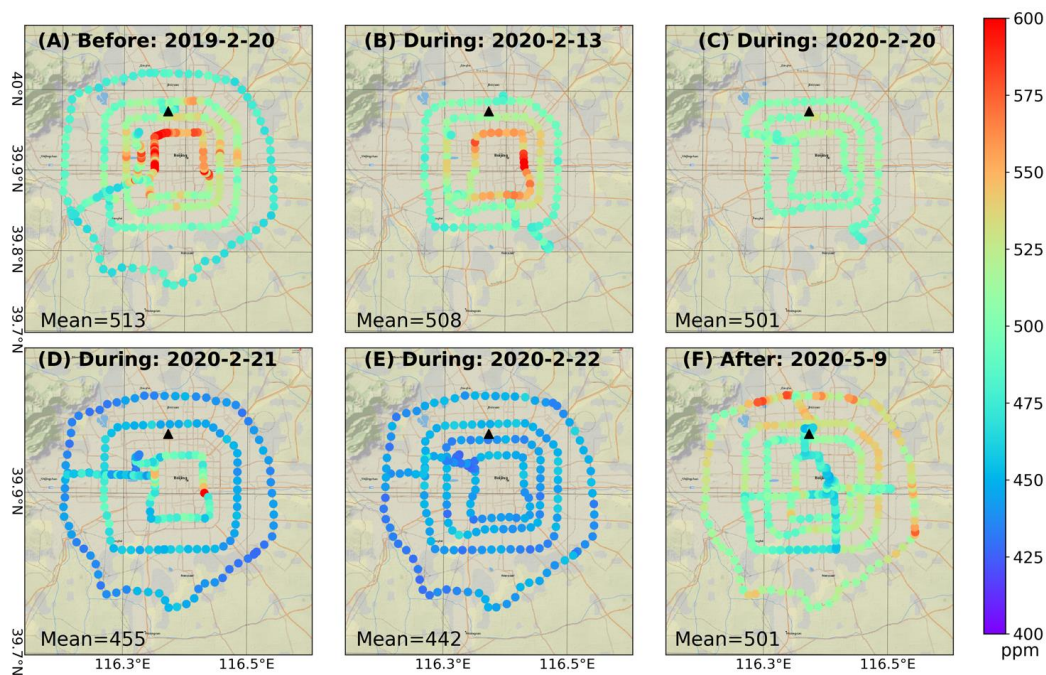


Figure 45. CO₂ concentration maps for six on-road trips. Circles are the locations of CO₂ concentration records taken at the 1-minute intervals averaged from data collected every 2 seconds (see methods). All sub-plots have the same colour barscale, ranging from 400 to 600 ppm. The black triangle is the location of the IAP tower. One trip (A: 20th February 2019) was conducted before the COVID-19 control restrictions, with an average of 513 (with an instrument uncertainty of ± 0.1) ppm. Four trips (B-E: 13th, 20th, 21st and 22nd February 2020) were conducted within during the COVID-19 control restrictions, with averages of 508 (± 1), 501 (± 1), 455 (± 1) and 442 (± 1) ppm and the total average CO₂ was 477, respectively ppm. One trip (F: 9th May 2020) was conducted after the COVID-19 control restrictions, with an average of 501 (± 5) ppm.

The CO₂ concentration maps of six on-road trips are shown in Figure 45. According to Table 1, we selected four trips as the trips with the most similar weather conditions: one BC trip (20th February 2019, Figure 4A), two DC trips (21st and 22nd February 2020, Figure 4D and 4E) and 1 AC trip (9th May 2020, Figure 4F). Statistically, the average of the 2 DC trips was 444 (± 1) ppm, which was 69 (± 1.1) and 57 (± 6) ppm lower than that of the BC and AC trips, respectively. The other two DC trips (13th and 20th February) were conducted on (lightly/heavily) polluted days, and the CO₂ concentrations on these two days were as high as those during the BC and AC trips.

We chose one DC trip (21st February 2020) for further analysis and compared it to the BC and AC trips. All three trips were conducted on clear days, and their trajectories were similar, from the outermost circle to the innermost circle, and covered one (morning or evening) rush hour. The difference was that the BC and DC trips hit the evening rush hour on the innermost ring road, whereas the AC trip hit the morning rush hour on the outermost ring road. This difference explained why the CO₂ concentration was high on the innermost road (2nd Ring Road) in figure 4A and 4D and on the outermost road (5th Ring Road) in figure 4F. The comparison of the three trips indicated that the CO₂ concentration in Figure 4D was lower than those in Figure 4A and 4F, and the statistics show that the mean CO₂ of the DC trips was approximately 58 (± 1.1) and 46 (± 6) ppm

带格式的：字体：倾斜

带格式的：上标

带格式的：上标

带格式的：上标

带格式的：下标

lower than those of the BC and AC trips, respectively. In addition, the average CO₂ concentration observed at the IAP tower during the same periods was much lower than the on-road observations (Figure 1B). These concentration differences (gradients) also implied that ground transportation emissions were a major CO₂ source on these urban roads.

However, it was difficult to completely eliminate the impact of background CO₂ fluctuations only through selecting trips with the most similar weather conditions. For example, the PBLHs during two DC trips with the most similar weather were 1587 m and 1113 m, which were almost twice of those during the BC and AC trips (Table 1). The CO₂ concentrations at the IAP tower also indicated that during these two DC trips, the CO₂ concentrations were 427 (± 0.1) and 428 (± 0.1) ppm, which were approximately 20 ppm lower than those for the BC and AC trips (in Figure 1). One trip was chosen as an example for BC (on 20th February 2019), DC (21st February 2020) and AC (9th May 2020) (shown in Figure 5A, 5D and 5F). All three trips were conducted on clear days, and their trajectories were similar that from the outermost circle to the innermost circle and covered one (morning or evening) rush hour. The difference was that the BC and DC trips hit the evening rush hour on the innermost circle road, whereas the AC trip hit the morning rush hour on the outermost circle. This difference explained the CO₂ concentration patterns (Figure 5A, 5D and 5F). The comparison of the three trips indicated that the CO₂ concentration measured in Figure 5D was intuitively lower than that in Figure 5A and 5F, and the statistics show that the DC CO₂ mean was approximately 58 and 46 ppm lower than that of the BC and AC trips, respectively. In addition, the average CO₂ concentration observed by the IAP tower during the same periods was much lower than the on road observations (Figure 2). These concentration differences (gradients) also implied that ground transportation emissions were a major CO₂ source on urban roads.

The other three DC trips (on 13th, 20th and 22nd February 2020) are shown in Figure 5B, 5C and 5E, with the averaged CO₂ concentrations of 508, 501 and 442 ppm. Due to background CO₂ concentration fluctuations (lightly polluted days), CO₂ concentrations on 13th and 20th February (Figure 5B and C) were as high as those during the BC and AC trips. Statistically, without considering the variation in the background CO₂ concentration, the average of the four DC trips was 477 ppm, which was 36 and 24 ppm lower than that of the BC and AC trips, respectively.

On-road CO₂ enhancement:

带格式的：下标

带格式的：下标

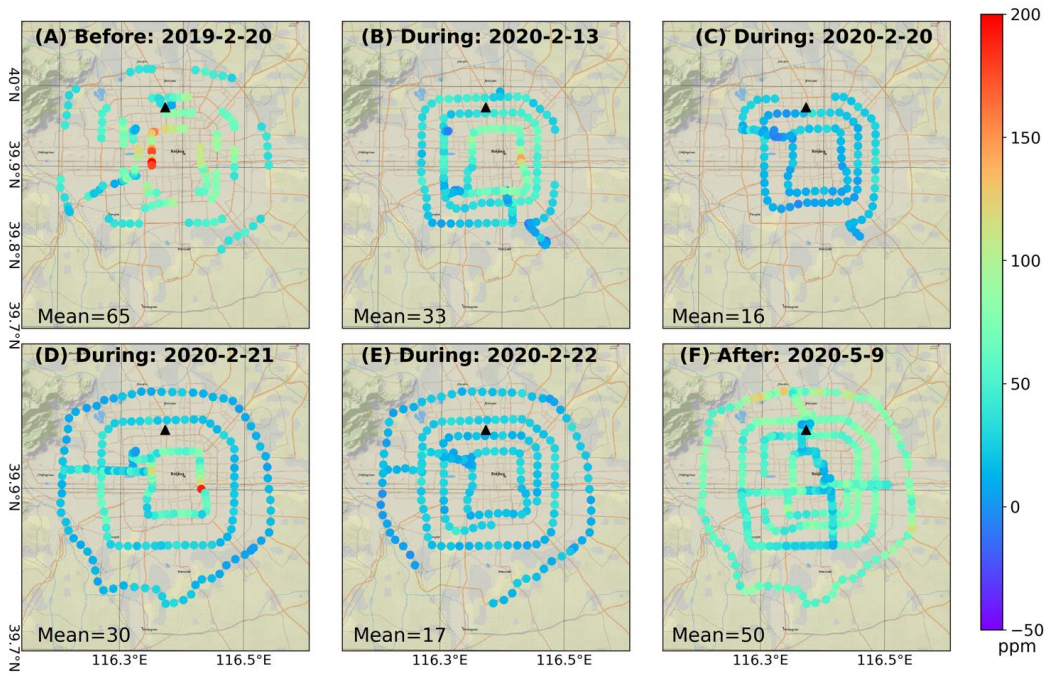


Figure 56. Maps of the CO₂ enhancement maps for all six trips using calculated by subtracting the IAP tower measurements from the on-road CO₂ measurements minus IAP tower measurements matched by time temporally. All sub-plots have the same colour bars scale, ranging from -50 to 200 ppm. One trip (A: 20th February 2019) was conducted before the COVID-19 restrictions, control with an average of 65 (± 0.2) ppm. Four trips (B-E: 13th, 20th, 21st and 22nd February 2020) were conducted within during the COVID-19 control restrictions, with averages of 33 (± 1.1), 16 (± 1.1), 30 (± 1.1) and 17 (± 1.1), and the total averaged CO₂ enhancement was 24 ppm, respectively. One trip (F: 9th May 2020) was conducted after the COVID-19 restrictions, control with an average of 50 (± 5.1) ppm.

To further reduce the influence of background CO₂ variations, we calculated the CO₂ enhancement for six trips by subtracting

Figure 6 shows the CO₂ enhancement maps of six trips, using the CO₂ concentration at IAP tower from the on-road CO₂ concentration minus those of IAP tower at the same time (shown in Figure 5). The spatial distribution patterns of the enhancement were similar to the distribution of the CO₂ concentration maps, in which the enhancements during rush hours were much higher for all trips. Furthermore, the refined spatial distribution of the CO₂ gradient implied emissions from ground transportation.

It is worth noting that the enhancements for the four DC trips were almost the same, although the weather conditions (based on the PBHL, PM_{2.5} and wind speed data) during these trips were quite different. However, the DC enhancements were obviously different from the BC and AC enhancements. During the two DC trips on polluted days (13th and 20th February 2020), the mean CO₂ concentrations were similar to those during the BC and AC trips (Figure 4B and 4C); however, the enhancements extracted the traffic emission signals from the background, with averages of 33 (± 1.1) and 16 (± 1.1) ppm (Figure 5B and 5C). Statistically, the average of the four DC enhancements was 24 (± 1.1) ppm, which was 41 (± 0.2) and 26 (± 6.2) ppm lower than those of the BC and AC enhancements.

The enhancements present a refined spatial distribution of the CO₂ concentration gradient, which implies ground transportation CO₂ emissions. As an example, Figures 6A, 6D and 6F presents the BC, DC and AC enhancement maps,

带格式的: 字体: 非加粗

带格式的: 字体: 非加粗

带格式的: 字体: 非加粗, 下标

带格式的: 字体: 非加粗

带格式的: 字体: 非加粗

带格式的: 字体: 非加粗

带格式的: 下标

带格式的: 字体: 非倾斜

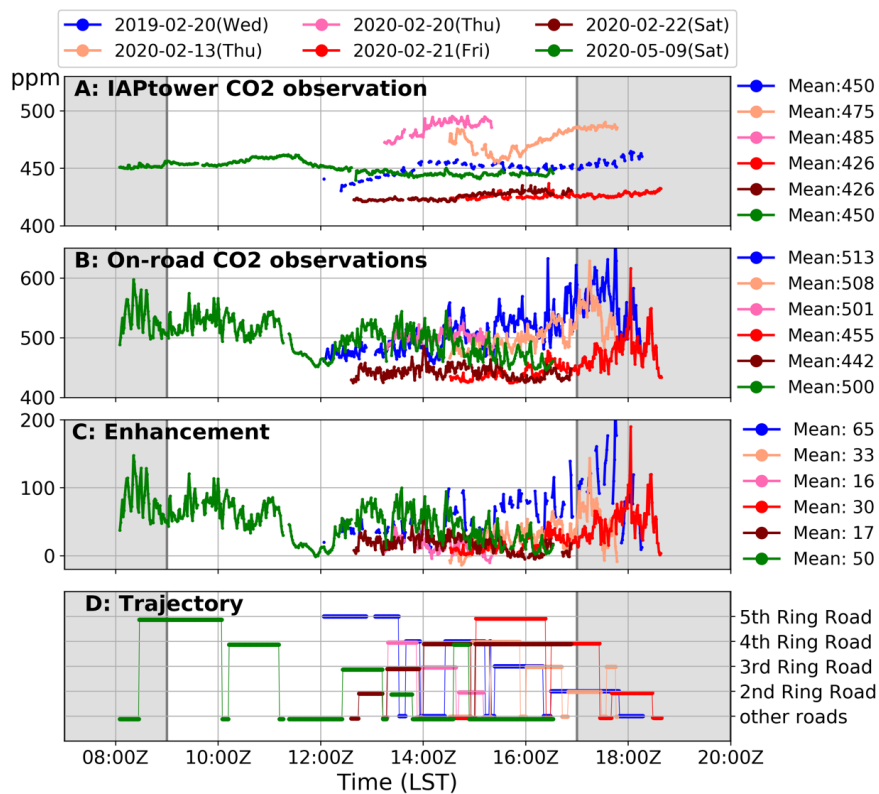
带格式的: 下标

305 respectively. Statistics show that enhancement during the DC trip was 30 ppm, which is 35 and 20 ppm lower than that
before and after this trip. The spatial distribution patterns of enhancement were similar to the CO₂ concentration maps, in
which enhancements during rush hours were much higher for all trips. Compared to the CO₂ concentration maps, the
310 enhancements showed important information in Figure 6B and 6C. The averaged CO₂ concentrations in these two trips were
similar to those during BC and AC (Figure 5B and 5C); however, the enhancements that extracted traffic emission signals
from the background, with averages of 33 and 16 ppm (Figure 6B and C), were much lower than those of BC and DC. The
enhancement maps also showed more useful information than the CO₂ concentration maps. For example, although the CO₂
315 concentration throughout the northern half of the 2nd Ring Roads was high (550–600 ppm) (Figure 5A), the enhancement
extracted more specific variations induced by traffic emissions in the northwest (Figure 6A). Generally, the statistical
enhancement the average of the four DC trips was 24 ppm, which was 41 and 26 ppm lower than that of the BC and AC trips,
respectively. Because of the IAP tower Picarro calibration and measurement procedure (see Method Section), there were
regular data gaps for the trip on 20th February 2019 (Figure 6A).

315 **Diurnal variation analysis:**

带格式的：删除线

带格式的: 左



带格式的: 字体: (默认) 宋体, 小四

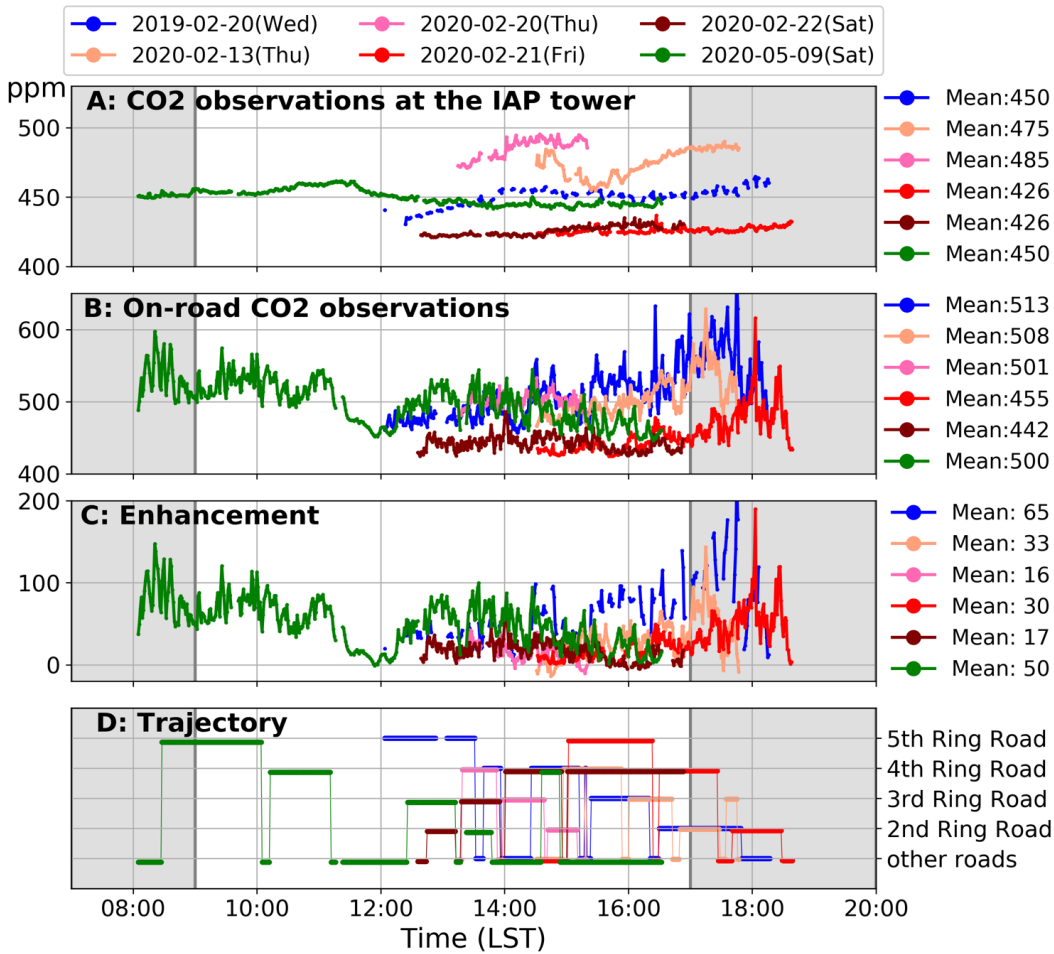


Figure 67. The six trips were plotted on a single day. The two grey regions refer to the morning and evening rush hours. The six colorful lines represent the six trips on different days. Four of the 6 trips covered at least one (morning/evening) rush hour. Panel A shows the CO₂ concentration from at the IAP tower during the trips. Panel B shows the on-road CO₂ concentration. Panel C shows the CO₂ enhancements. Panel D shows the six trip trajectories.

Figure 67 shows the diurnal variation from in the CO₂ concentrations from IAP tower observations. CO₂ concentrations, on-road CO₂ concentrations, enhancements and trajectories for all trips. In Figure 67A, the IAP tower CO₂ concentration measured at the IAP tower concentrations were relatively stable, and stable and showed the an difference approximate 50 ppm difference between trips. The CO₂ concentrations at the IAP tower CO₂ concentrations during the first two DC trips the two trips during COVID-19 (13th and 20th February 2020) were ~30 ppm higher than those during the BC and AC trips. However, the CO₂ concentrations concentrations during the other two DC trips (21st and 22nd February 2020) were ~20 ppm lower than those during the those during the BC and AC trips. These “baseline” CO₂ concentration fluctuations make the on-road observations not directly comparable directly. In Figure 78B, the CO₂ concentrations show a “double-peak” pattern, with peaks during within the morning (7:00-9:00) and evening rush hours (17:00-20:00) rush hours. During the rush hours, the CO₂ concentrations ranged from 500 to 600 ppm, which were approximately 100 ppm higher than the concentrations during working hours (9:00-17:00). The comparison of BC and AC indicates that the CO₂ concentrations measured on 13th and 20th February 2020 did not significantly decrease during 12:00-17:00. However, the CO₂

带格式的: 下标

335 concentrations measured on 21st and 22nd February 2020 were much lower (~50 ppm) than those measured during the BC
 and AC trips. This difference is consistent with the spatial distribution mentioned before and is most likely due to ~~the CO₂~~
~~concentration~~-background CO₂ fluctuations.

340 In Panel C, all DC CO₂-enhancements were generally lower than ~~the those of~~ BC and AC ~~enhancements, and the statistics~~
~~for different time periods are listed in Table 3.~~ However, we ~~still also~~ found ~~verysmall~~ ~~low~~-enhancements ~~values~~ for BC
 and AC, ~~similar to those for DC.~~ For example, ~~the~~ AC enhancement at ~~approximately~~ 12:00 ~~and~~ 16:00 was almost the
 same as ~~the that of~~ DC ~~enhancement at that time.~~ ~~By examining the~~ ~~With the help of~~ trip routes (Panel D), we found that
 during that period, the on-road observation vehicle was not driving on the main ring roads. ~~As another example, is the~~ BC
 345 ~~enhancement at approximately~~ 18:00, ~~which~~ indicates that the enhancement decreased in a stepwise manner, also because the
 vehicle drove on other roads (Panel D). ~~In Panel C, all DC CO₂ enhancements were generally lower than those of BC and~~
~~AC, and the statistics for different time periods are also listed in Table 3.~~

Table 3. ~~Statistical analysis of~~ CO₂ enhancement (mean and instrumental uncertainties) for six trips ~~over different periods~~
 (ppm)

<u>Label</u>	<u>Observation</u> <u>date</u>	<u>Observation</u> <u>condition</u>	<u>Total</u> <u>Weather</u> <u>average</u> <u>enhancement</u> <u>(07:00-20:00)</u>	<u>Morning</u> <u>Total</u> <u>RUSHrush</u> <u>average</u> <u>hours</u> <u>(07:00-09:00)</u> <u>(07:00-09:00)</u>	<u>Morning</u> <u>Weather</u> <u>RUSHhours</u> <u>(07:00-09:00)</u>	<u>Evening</u> <u>Weather</u> <u>RUSHrush</u> <u>hours</u> <u>(09:00-17:00)</u> <u>(17:00-20:00)</u>	<u>Evening</u> <u>RUSHhours</u> <u>(17:00-20:00)</u>
<u>BC</u>	<u>2019-2-20</u> <u>(Wed)</u>	<u>2019-2-20</u> <u>(Wed)</u> <u>Clear</u>	<u>65</u> <u>(±0.2)</u>	<u>65</u> <u>=</u>	<u>-</u> <u>54</u> <u>(±0.2)</u>	<u>54</u> <u>100</u> <u>(±0.2)</u>	<u>100</u>
<u>DC</u>	<u>2020-2-13 (Thu)</u>	<u>2020-2-13 (Thu)</u> <u>Stable/light</u> <u>pollution</u>	<u>33</u> <u>(±1.1)</u>	<u>22</u> <u>=</u>	<u>26</u> <u>(±1.1)</u>	<u>55</u> <u>26</u> <u>(±1.1)</u>	<u>55</u>
<u>DC</u>	<u>2020-2-20 (Thu)</u>	<u>2020-2-20 (Thu)</u> <u>Stable/light</u> <u>pollution</u>	<u>16</u>	<u>16</u>	<u>-</u>	<u>16</u>	<u>-</u>
	<u>2020-2-21 (Fri)</u>	<u>2020-2-21 (Fri)</u> <u>Windy day</u>	<u>20</u>	<u>20</u>	<u>-</u>	<u>16</u>	<u>50</u>
	<u>2020-2-22 (Sat)</u>	<u>2020-2-22 (Sat)</u> <u>Windy day</u>	<u>17</u>	<u>17</u>	<u>-</u>	<u>17</u>	<u>-</u>
<u>AC</u>	<u>2020-2-9 (Sat)</u>	<u>2020-2-9 (Sat)</u> <u>Windy day</u>	<u>50</u>	<u>50</u>	<u>80</u>	<u>46</u>	<u>-</u>
	<u>Total BC-DC</u>			<u>41</u>	<u>-</u>	<u>35</u>	<u>48</u>
	<u>Total AC-DC</u>			<u>26</u>	<u>-</u>	<u>27</u>	<u>-</u>

vy pollution

	<u>2020-2-20 (Thu)</u>	<u>Stable/light pollution</u>	<u>16 (±1.1)</u>	=	<u>16 (±1.1)</u>	=
	<u>2020-2-21 (Fri)</u>	<u>Windy day</u>	<u>30 (±1.1)</u>	=	<u>16 (±1.1)</u>	<u>50 (±1.1)</u>
	<u>2020-2-22 (Sat)</u>	<u>Windy day</u>	<u>17 (±1.1)</u>	=	<u>17 (±1.1)</u>	=
<u>AC</u>	<u>2020-5-9 (Sat)</u>	<u>Windy day</u>	<u>50 (±5.1)</u>	<u>80 (±5.1)</u>	<u>46 (±5.1)</u>	=
	<u>Total BC-DC</u>		<u>41 (±1.3)</u>	=	<u>35 (±1.3)</u>	<u>48 (±1.3)</u>
	<u>Total AC-DC</u>		<u>26 (±6.2)</u>	=	<u>27 (±6.2)</u>	=

350

The ~~average of CO₂ mean~~ enhancement ~~for~~ the whole BC trip was 65 (±0.2) ppm, and the average for ~~the the~~ evening rush hours (100 ~~-~~ ±0.2 ppm) was two times that ~~of for~~ the working hours (54 ±0.2 ppm). This result implies that the increase in vehicle volume ~~in during~~ the evening rush hours leads to large traffic emissions and an increase in the on-road CO₂ concentration. For DC, all trips covered the working hours, with a low enhancement of approximately 20 ppm. There was not obvious difference between weekdays and weekends during ~~this period working hours, which indicated that there was no "week effect"~~. The reason may ~~be that because~~ the government encouraged people to work remotely at home. Therefore, even on weekdays, ~~according to traffic conditions,~~ the commute ~~volume was low was small~~ (SFigure 2). Among these four trips, two (on 13th and 20th February 2020) covered the evening rush hours with high averaged enhancements of 55 (±1.1) and 50 (±1.1) ppm. Therefore, the total ~~average~~ enhancements ~~averages for~~ these two trips were higher than those ~~for of~~ the other two trips, which covered ~~only only~~ working hours. For AC, on 9th May 2020, although it was a Saturday, many residents chose to go out of town for ~~the~~ weekends. The morning rush hours still existed, with a high enhancement of 80 (±5.1) ppm, and then during the working hours, the enhancement decreased to 46 (±5.1) ppm.

355

360

365

370

375

380

The comparison of trips showed that the averaged CO₂ enhancement ~~for the from 4 whole~~ DC trips was 41 (±1.3) and 26 (±6.2) ppm lower than that ~~from for~~ the BC and AC trips, respectively. ~~Compared to the BC trip,~~ the averaged AC enhancement was ~~15-15 (±5.3)~~ ppm lower ~~than the average BC enhancement~~. This difference may be caused by two factors: 1) ~~The first relates to "weekly effects"; as previously mentioned,~~ a previous study also suggested that, compared to ~~that during~~ weekdays, the average daily traffic CO₂ emissions during weekends in the north part of the fifth Ring Road (LinCui Road - Anli Road, 3 km) decreased by 5% ~~throughout whole in~~ 2014 ~~according to the Motor Vehicle Emission Simulator model (from 131.74 t/d to 126.33 t/d)~~ (Zheng et al., 2020); 2) ~~until Until~~ 9th May 2020, although there were approximately 30 days without ~~increased increases in~~ COVID-19 cases in Beijing, the city was still under Level-2 response control; social life was recovering, but had not yet completely recovered.

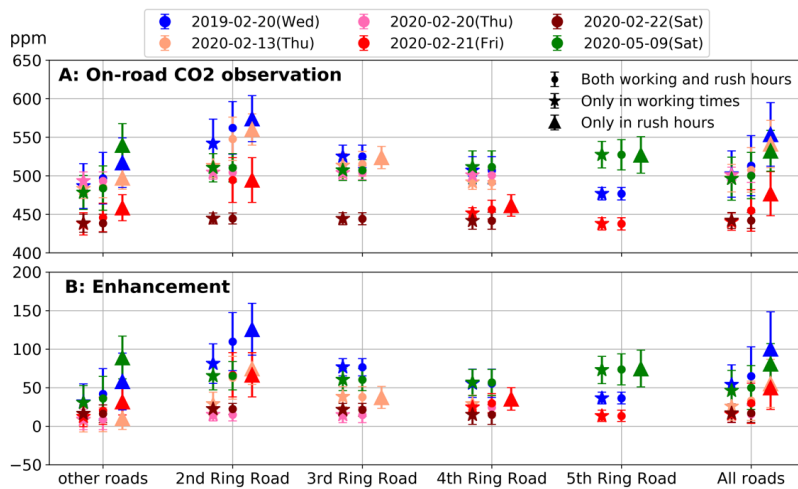
Analysis of CO₂ enhancement ~~on for~~ independent time periods and roads:

According to the previous analysis, we found that enhancement exhibited a strong correlation with ~~the~~ time (rush or working hours) and road types. Therefore, we statistically analyzed ~~the~~ CO₂ enhancements according to ~~the~~ road types and time periods, as shown in Figure 7. In Figure 7A, on 13th and 20th February 2020, the CO₂ concentrations on the other, 2nd, and 4th ~~Ring R~~ Roads and all roads were at the same levels as those during the BC and AC trips. However, in Figure 7B, ~~the the~~ enhancement showed that ~~the four DC enhancements four trips during COVID-19~~ were generally lower than those during AC and BC for all road types. Although on the 2nd Ring Road, the DC ~~trips enhancements~~ on 13th and 21st February 2020 were

385
390

almost the same as the BC and AC trips enhancements, the DC trips were during rush hours, whereas the AC and BC trips were during working hours. Some very high deviations also occurred (rush hours on the other roads, 2nd and 5th Ring roads), which indicates the dispersion of the CO₂ enhancement. The reason for this difference is that we classified all roads excluding the ring roads as other roads, which may have included arterial and residential roads, so the different road types may have increased the deviation. For the 2nd and 5th Ring-ring roads, high deviation occurred because during rush hour, traffic flow and transportation varied greatly and resulted in drastic changes in the CO₂ enhancement, which also caused much higher deviations. We also calculated specific statistics, which are listed in Table 4. After a statistical significance test, we found that the CO₂ enhancement difference between working times and rush hours for all trips was significant ($p < 0.02$, assuming that $\alpha=0.05$). The CO₂ enhancement for BC was also significantly different from that for DC ($p < 0.05$); however, the difference between the AC and BC enhancements was not significant. This suggests that the decreased CO₂ enhancement observed during the COVID-19 restrictions was significantly different from those before and after the COVID-19 restrictions. We also calculated specific statistics, which are listed in Table 4.

带格式的: 下标
带格式的: 下标
带格式的: 下标



395

Figure 78. Statistically analysis (mean and one standard deviation) of all on-road trips according to the road types and times. Panel A shows the on-road CO₂ concentration. Panel B shows the CO₂ enhancement.

Table 4. Statistical analysis (mean/one standard deviation) of the CO₂ enhancement for six trips according to the times and road types

Label	date	Time	Other roads	2nd Ring Road	3rd Ring Road	4th Ring Road	5th Ring Road	All roads	Significance test (p)	
									Working hours compared to rush hours	DC/AC compared to BC
BC	2019-2-20 (Wed)	Working hours	31/±24	81/±26	77/±11	56/±18	37/±8	54/±26	=	=
		Rush hours	58/±37	125/±34	-	-	-	100/±48	0.015	=
		Both	42/±33	109/±38	77/±11	56/±18	37/±8	65/±38	=	=
DC	2020-2-13 (Thu)	Working hours	8/±16	29/±15	38/±13	29/±11	-	26/±18	0.018	=

带格式的: 字体: 8 磅
带格式的: 字体: 8 磅
带格式的: 字体: 8 磅

		Rush hours	10 _{±14}	74 _{±20}	37 _{±14}	-	-	55 _{±31}	=
		Both	9 _{±16}	63 _{±28}	38 _{±13}	29 _{±11}	-	33 _{±26}	= 0.041
2020-2-20 (Thu)		Working hours	9 _{±13}	15 _{±8}	14 _{±10}	24 _{±8}	-	16 _{±11}	=
		Rush hours	-	-	-	-	-	-	=
		Both	9 _{±13}	15 _{±8}	14 _{±10}	24 _{±8}	-	16 _{±11}	= 0.001
2020-2-21 (Fri)		Working hours	12 _{±13}	-	-	25 _{±7}	13 _{±7}	16 _{±10}	= 0.002
		Rush hours	32 _{±17}	67 _{±29}	-	35 _{±15}	-	50 _{±28}	=
		Both	20 _{±18}	67 _{±29}	-	30 _{±13}	13 _{±7}	30 _{±26}	= 0.026
2020-2-22 (Sat)		Working hours	16 _{±11}	22 _{±7}	21 _{±8}	15 _{±13}	-	17 _{±12}	=
		Rush hours	-	-	-	-	-	-	=
		Both	16 _{±11}	22 _{±7}	21 _{±8}	15 _{±13}	-	17 _{±12}	= 0.001
AC 2020-5-9 (Sat)		Working hours	30 _{±22}	65 _{±18}	60 _{±14}	57 _{±17}	73 _{±18}	46 _{±26}	= 0.008
		Rush hours	89 _{±28}	-	-	-	75 _{±24}	81 _{±26}	=
		Both	36 _{±29}	65 _{±18}	60 _{±14}	57 _{±17}	73 _{±20}	50 _{±28}	= 0.41

Discussion:

Analysis of the correlation analysis with traffic flow:

It was difficult to obtain a quantitative evaluation of the influence of COVID-19 restrictions on CO₂ emissions from traffic during our study period because there were of limited data. In this study, we found that the one-trip enhancement during for DC (on 21st February 2020, with the most similar weather conditions and a -and route that were the most similar to those for the BC and AC trips) as trips during BC and AC) was 30 (±1.1) -ppm. The enhancement accounted for 46% of that during for BC (65 ±0.2 -ppm), and the enhancement during for AC (50 ±5.1 ppm) accounted for 77% of that for during-BC. Here, we adopted four datasets and methods to explain our hypothesis that the decrease in traffic volume led to a reduction in on-road CO₂ emissions and concentration during the COVID-19 control/restrictions. First, according to the “analysis of road traffic operation in Beijing during COVID-19 in 2020” published by the Beijing Transport Institute, during the first 8 weeks (from 1st February to 31st March, the DC period in this study), the Beijing ground transportation index (calculated based on the ratio of congestion-congested road length to the and-whole road length) decreased by 53% compared to that on to-normal days, -whereas, during 1st April to 31st May, the index recovered to 92%. (Zhang, 2020). The index implied that traffic flow of for DC is was dramatically decreased compared to that of for BC, and the index for AC almost recovered almost-but not completely. This index variation is consistent with our observations -results. Second, two remote sensing images from similar dates were adopted (Figure 89). According to statistics and estimations based on coverage area, we found that the BC traffic flows on the main roads of the 4th and 3rd Ring Roads are were 227 and 226 veh/km (vehicles per kilometere), respectively. However, the DC traffic flow decreased to 35 and 34 veh/km, with-reflecting a reduction of approximately 85%. Simply With the assuming that emission factors were the same, the CO₂ emissions on roads during for DC may have sharply

420 decreased by approximately 85% compared to those ~~during for~~ BC. This difference is higher than the passenger
 transportation decrease estimated by Han *et al.*'s (Han *et al.*, 2020) (56.6% in the first quarter of 2020) because ~~the~~ remote
 sensing images ~~is are a~~ snapshots and ~~cover only~~ part of the urban area. ~~Moreover,~~ and Hans' results are the average of the
 first three months and the entire Beijing administrative region. Third, we also ~~used~~ ~~collected real time~~ traffic congestion
 conditions ~~data, although with low temporal and spatial resolution, to indicate the on-road traffic flow and emissions (Figure~~
 425 ~~9)(for each road), road name, geographic information, road type and average speed for one hour data from the Autonavi~~
~~Open Platform (https://lbs.amap.com/). The data, although with low temporal and spatial resolution, could be used to show~~
~~traffic conditions on roads, and then indicate the on road traffic flow and emissions (Figure 10).~~ Fourth, the vehicle speed
 maps of ~~the~~ six trips were ~~also~~ plotted (Figure 10). Overall, these maps reflect the spatial patterns of road traffic conditions
 during the surveys and could also reflect the specifics on a single road. However, these maps are ~~subject-sensitive~~ to
 430 subjective speed variations caused by drivers, such as when facing traffic lights.

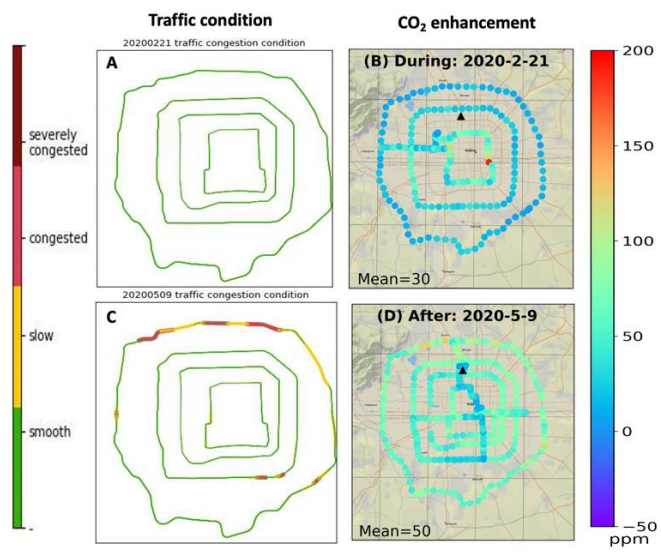
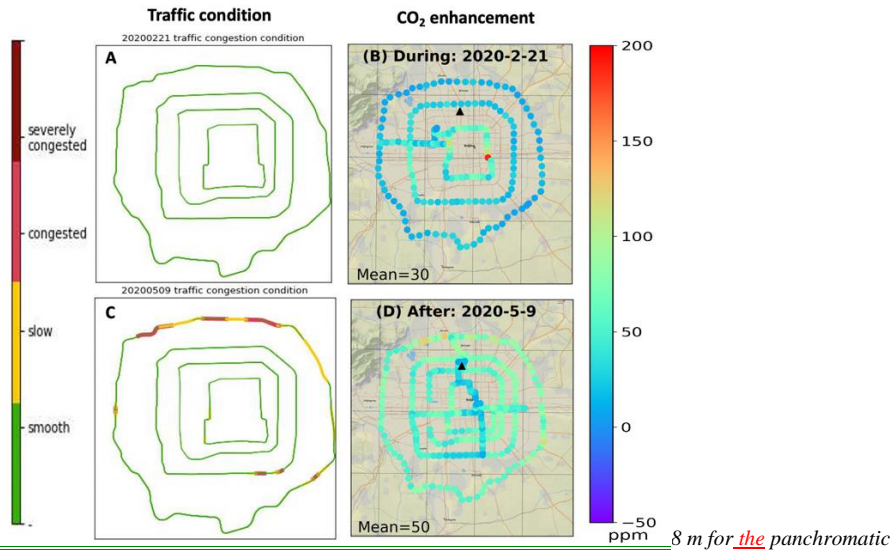
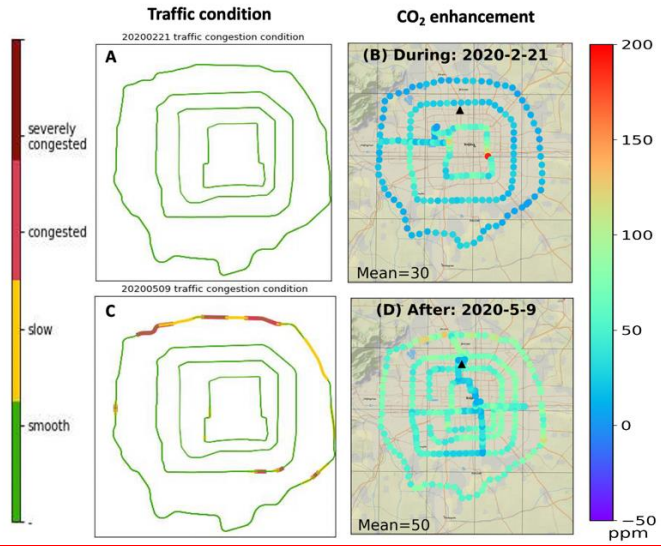


Figure 89. Traffic volume comparison ~~by-with~~

435 using remote sensing images. (A) Coverage region of remote sensing images (purple polygon) and example region shown on
 the right (red square); (B) remote sensing images from Google Earth on 21st February 2019 at 11:42:00 (LST), with a
 spatial resolution of 0.37 m for multispectral band image; 61 vehicles on the main road were interpreted (labelled by blue
 polygons); (C) remote sensing image from ~~the~~ Beijing-2 satellite on 19th February 2020 at 10:20:08 (LST), with a spatial



resolution of 0.8 m for the panchromatic band images and 24 vehicles labelled with red polygons.



带格式的: 居中

带格式的: 左

Figure 940. Comparison of traffic conditions comparison with the CO₂ enhancement. (A) Traffic conditions on 21st February 2020; (B) CO₂ enhancement on 21st February 2020; (C) traffic conditions on 9th May 2020; (D) CO₂ enhancement on 9th May 2020.

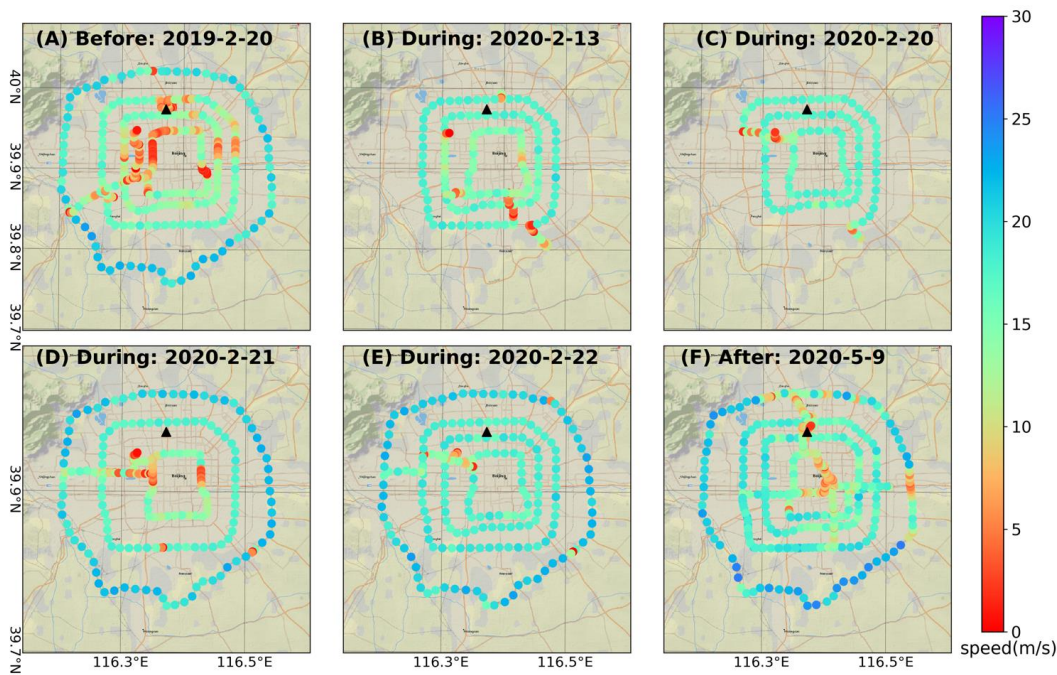


Figure 10. Speed maps of six trips, ranging from 0 to 30 m/s. One trip (A: 20th February 2019) was conducted before the COVID-19 control restrictions. Four trips (B-E: 13th, 20th, 21st and 22nd February 2020) were conducted during the COVID-19 restriction control; one trip (F: 9th May 2020) was conducted after the COVID-19 restriction control.

Uncertainty analysis:

In this research, ~~The~~ uncertainty of this research mainly existed in the following terms:

(1) Uncertainty from the observation instruments.

In this study, four instruments were adopted for measuring CO₂ concentrations; three for on-road observations (a Picarro G2401, with an accuracy of approximately 0.1 ppm; a LI-COR LI-7810, ~1 ppm; and a low-cost sensor, no more than 5 ppm) and one for the IAP tower observation (Picarro G2301, ~0.1 ppm). During analysis, both the proposed enhancement method and the CO₂ concentration/enhancements of different trips were compared using linear analysis (addition/subtraction).

Therefore, the enhancement uncertainties from the observation instruments were: ~0.2 ppm for BC, ~1.1 ppm for DC, less than 5.1 ppm for AC, ~1.3 ppm for comparing BC and DC, and less than 6.2 ppm for comparing DC and AC. Note that the standard deviations shown in Table 4 mainly presented CO₂ concentration fluctuations within specific periods and on certain roads and uncertainty from instruments, (relatively small).

(+)(2) The IAP tower CO₂ concentration was used as the background ~~in~~ from Beijing.

In this study, the IAP tower data were adopted as the urban background CO₂ concentration in Beijing. Its measurement footprint was influenced by two factors: wind speed/direction and air intake height. For wind speed/direction, in Beijing, the main wind directions were northwest (winter) and southeast (summer) (Cheng et al., 2018). However, IAP tower data were collected from different levels, as described in the method section. Generally, high-level data would have a large footprint and good representativeness and cover large regions. For example, Cheng et al. (Cheng et al., 2018) showed that CO₂ data recorded at 280 m height-level CO₂ data have an averaged fetch of ~17 km, which may covers a major part of the city; data collected at 80 m height-level data have an averaged fetch of ~8 km; data collected at and 8 m height-level data may have

- 带格式的: 字体: (默认) Times New Roman, 10 磅
- 带格式的: 下标
- 带格式的: 字体: (默认) Times New Roman, 10 磅
- 带格式的: 字体: (默认) Times New Roman, 10 磅
- 带格式的: 字体: (默认) Times New Roman, 10 磅
- 带格式的: 字体: (默认) Times New Roman, 10 磅
- 带格式的: 字体: (默认) Times New Roman, 10 磅
- 带格式的: 下标
- 带格式的: 字体: (默认) Times New Roman, 10 磅
- 带格式的: 下标
- 带格式的: 字体: (默认) Times New Roman, 10 磅
- 带格式的: 字体: (默认) Times New Roman, 10 磅
- 带格式的: 字体: (默认) Times New Roman, 10 磅
- 带格式的: 字体: (默认) Times New Roman, 10 磅
- 带格式的: 字体: (默认) Times New Roman, 10 磅
- 带格式的: 字体: 非倾斜

475
480
485
490
495
500
505
510
515

an average fetch of only ~230 m; and the fetch at the surface level (2 m) may be smaller. Therefore, there are two uncertainties. The first is the height variation during the observation trips. Due to the data availability and for comparison consistency, we chose the lower- and surface-level data. According to Cheng *et al.* (2018), the CO₂ concentration at the 80 m height is ~15 ppm higher than that at the 8 m height. Therefore, if this difference between the lower level and surface level was added, the BC enhancement would increase (~15 ppm), which means that the DC enhancement would be even lower (~56 ppm) than the BC enhancement. The other is the difference between the surface level data and 280-metre height data in different seasons. Due to the data availability and comparison consistency, we chose the lower and surface level data. According to Cheng *et al.* (2018), the CO₂ concentration at the 80 m height level is ~15 ppm higher than that at 8 m. Therefore, adding this difference between the lower level and surface level, the BC enhancement would increase (~15 ppm), which means that the DC enhancement would be even lower (~56 ppm) than the BC enhancement. According to Cheng *et al.* (2018), the monthly averaged CO₂ showed a relatively stable difference among the different heights: the CO₂ at the lower level was approximately 40 ppm higher than that at 280-metres in February and approximately 30 ppm higher in May. The AC enhancement should increase 10 ppm additionally, which means that the DC enhancement would be even lower (~36 ppm) than the AC enhancement. Considering these uncertainties, the results support is consistent with our hypothesis.

(3) Influences of vegetation sinks and natural changes.

To understand the CO₂ variability impacted by natural sinks (especially for vegetation), we used the dynamic vegetation and terrestrial carbon cycle model VEGAS (Zeng *et al.*, 2014) to simulate the terrestrial biosphere-atmosphere flux (F_{ta}) in Beijing during 2000-2020 (SFigure 3). The model was run at a 2.5×2.5-degree resolution from 1901 to June 2020, forced by observed climate variables, including monthly precipitation and hourly temperature. Although precipitation and temperature in 2020 were higher than the climatology (average of last 20 years), the difference between the F_{ta} in 2020 and the average was within one standard deviation. This suggests that the F_{ta} in 2020 was not obviously unusual compared to that over the last 20 years. We also analysed the CO₂ concentration at the Shangdianzi station in the Beijing rural region, which is one of the three WMO/GAW regional stations in China, to determine the CO₂ background variation (Fang *et al.*, 2016). The results (SFigure 4) showed that the background CO₂ concentration variation mainly induced by natural factors from February to May was only approximately 5 ppm. However, these two factors (vegetation flux and natural changes) both indicate areas far larger than Beijing urban areas. Because the location of the IAP tower and the tracks of the on-road observations are both in urban Beijing and we used the enhancement method, these factors were reduced.

(4) When data were collected, especially when switching between lower and upper levels, a large amount of data was lost. However, because the data gaps were evenly distributed and the IAP tower CO₂ concentrations were relatively stable, we assumed that it would not affect the final statistical results.

(5) In this study, our on-road observations did not have a fixed route or beginning/ending time, which means that the observations on different dates represented different roads. Therefore, we analyzed-analysed a wide time range of observations (rush hours, working hours or whole days), which may have also caused uncertainty.

Conclusion

The CO₂ emission reduction caused by COVID-19 restrictions is an opportunity to test our ability to collect CO₂ observations in urban regions. In this study, we chose on-road CO₂ concentrations as the target, because ground transportation is the main source of CO₂ in urban areas and was remarkably influenced by policy restrictions due to the COVID-19 pandemic. We conducted six on-road observations in Beijing, including one trip before COVID-19 restrictions, in February 2019; four trips during COVID-19 restrictions, in February 2020; and one trip in May 2020, after COVID-19 restrictions had been eased, aiming at traffic emissions, which the potentially represents the largest reduction source in urban areas due to COVID-19, we conducted six on-road observations in Beijing, China. The results showed that on-road CO₂ concentrations were strongly affected by traffic emissions and weather. However, the enhancement metric, which was the

- 带格式的: 字体: (默认) Times New Roman, 10 磅
- 带格式的: 字体: (默认) Times New Roman, 10 磅
- 带格式的: 字体: (默认) Times New Roman, 10 磅
- 带格式的: 字体: (默认) Times New Roman, 10 磅
- 带格式的: 字体: (默认) Times New Roman, 10 磅
- 带格式的: 字体: (默认) Times New Roman, 10 磅
- 带格式的: 字体: (默认) Times New Roman, 10 磅
- 带格式的: 字体: (默认) Times New Roman, 10 磅
- 带格式的: 字体: (默认) Times New Roman, 10 磅, 非倾斜
- 带格式的: 字体: (默认) Times New Roman, 10 磅
- 带格式的: 字体: (默认) Times New Roman, 10 磅, 非上标/下标
- 带格式的
- 带格式的
- 带格式的
- 带格式的
- 带格式的
- 带格式的: 下标
- 带格式的: 下标
- 带格式的
- 带格式的
- 带格式的
- 带格式的
- 带格式的
- 带格式的
- 带格式的
- 带格式的
- 带格式的
- 带格式的
- 带格式的
- 带格式的
- 带格式的
- 带格式的: 下标
- 带格式的
- 带格式的: 下标
- 带格式的: 下标
- 带格式的: 下标
- 带格式的: 下标

difference ~~of in the~~ on-road CO₂ concentration and the city “background”, reduced the impact of background CO₂ fluctuations. The results showed that ~~during for DC~~ COVID-19, the total average CO₂ enhancements of the four trips were 41 (~~±1.3~~) ppm and 26 (~~±6.2~~) ppm lower than those ~~before and after for BC and AC~~, respectively. Detailed analysis showed that this reduction commonly existed on all road types during the same time period (rush hours/working hours). ~~For the DC trips, During COVID-19,~~ there was no significant difference ~~during work hours~~ between weekdays and weekends. ~~During rush hours,~~ the enhancements ~~during rush hours~~ were much higher than those during working hours, and compared with ~~the enhancement reduction during rush hours for BC, that for the DC~~ enhancements ~~reduction during rush hours~~ was most obvious. Our findings, which show a clear decrease ~~during for DC~~ compared with ~~those during~~ BC and AC, are consistent with the COVID-19-~~restriction~~ ~~control~~, which may be direct evidence of reductions in CO₂ concentrations and carbon emissions. On-road CO₂ observations are an effective way to understand and ~~analyze the~~ urban carbon CO₂ concentration distribution and variation and should be regularly and more frequently conducted in future work. ~~With the~~ development and successful application of ~~the~~ miniaturized and low-cost CO₂ monitoring instruments used in this study (Khan et al., 2012; Shusterman et al., 2016; Martin et al., 2017; Mueller et al., 2020; Bao et al., 2020), ~~these instruments~~ will greatly ~~aid in the help~~ collection of on-road observations and even high-density network observations and play a key role in future urban carbon observations.

Author contributions

Pengfei Han, Bo Yao and Ning Zeng conceived and designed the study. Di Liu summarized the results and wrote the draft of the paper. Wanqi Sun and Pengfei Han designed and conducted the on-road observations. Pucai Wang provided the IAP tower observation data. Ke Zheng, Zhiqiang Liu, Han Mei and Qixiang Cai helped to collect, process and ~~analyze~~ ~~analyse~~ data.

Competing interests.

The authors declare that they have no conflicts of interest.

Acknowledgements:

This work was supported by the National Key R&D Program of China (No. 2017YFB0504000). Special thanks are given to Zhe Hu, Zhimin Zhang and Xiaoli Zhou for collecting ~~the~~ data and conducting the observations.

References:

1. Bao, Z., Han, P., Zeng, N., Liu, D., Cai, Q., Wang, Y., Tang, G., Zheng, K., and Yao, B.: Observation and modeling of vertical carbon dioxide distribution in a heavily polluted suburban environment, Atmospheric and Oceanic Science Letters, 13, <https://doi.org/10.1080/16742834.2020.1746627>, 2020.
2. Bush, S. E., Hopkins, F. M., Randerson, J. T., Lai, C. T., and Ehleringer, J. R.: Design and application of a mobile ground-based observatory for continuous measurements of atmospheric trace gas and criteria pollutant species, Atmospheric Measurement Techniques, 8, 3481-3492, 10.5194/amt-8-3481-2015, 2015.
3. Cheng, X. L., Liu, X. M., Liu, Y. J., and Hu, F.: Characteristics of CO₂ Concentration and Flux in the Beijing Urban Area, Journal of Geophysical Research-Atmospheres, 123, 1785-1801, 10.1002/2017jd027409, 2018.
4. Fang, S. X., Tans, P. P., Dong, F., Zhou, H., and Luan, T.: Characteristics of atmospheric CO₂ and CH₄ at the Shangdianzi regional background station in China. Atmospheric Environment, 131, 1-8, 2016.
5. Friedlingstein, P., Jones, M. W., O'Sullivan, M., Andrew, R. M., Hauck, J., Peters, G. P., Peters, W., Pongratz, J., Sitch, S., Le Quere, C., Bakker, D. C. E., Canadell, J. G., Ciais, P., Jackson, R. B., Anthoni, P., Barbero, L., Bastos, A., Bastrikov, V., Becker, M., Bopp, L., Buitenhuis, E., Chandra, N., Chevallier, F., Chini, L. P., Currie, K. I., Feely, R. A., Gehlen, M., Gilfillan, D., Gkritzalis, T., Goll, D. S., Gruber, N., Gutekunst, S., Harris, I., Haverd, V., Houghton, R. A., Hurtt, G., Ilyina, T., Jain, A. K., Joetzjer, E., Kaplan, J. O., Kato, E., Goldewijk, K. K., Korsbakken, J. I.,

带格式的: 编号 + 级别: 1 + 编号样式: 1, 2, 3, ... + 起始编号: 1 + 对齐方式: 左侧 + 对齐位置: 0 厘米 + 缩进位置: 0.74 厘米

带格式的: 字体: (默认) Times New Roman

域代码已更改

带格式的: 字体: (默认) Times New Roman

带格式的: 字体: (默认) Times New Roman

带格式的: 字体: (默认) Times New Roman, 字体颜色: 自动设置, 不检查拼写或语法, 图案: 清除

带格式的: 字体: (默认) Times New Roman, 字体颜色: 自动设置, 不检查拼写或语法, 图案: 清除

带格式的: 字体: (默认) Times New Roman, 字体颜色: 自动设置, 不检查拼写或语法, 图案: 清除

带格式的: 编号 + 级别: 1 + 编号样式: 1, 2, 3, ... + 起始编号: 1 + 对齐方式: 左侧 + 对齐位置: 0 厘米 + 缩进位置: 0.74 厘米

带格式的: 字体: (默认) Times New Roman

Landschuetzer, P., Lauvset, S. K., Lefevre, N., Lenton, A., Lienert, S., Lombardozzi, D., Marland, G., McGuire, P. C., Melton, J. R., Metz, N., Munro, D. R., Nabel, J. E. M. S., Nakaoka, S.-I., Neill, C., Omar, A. M., Ono, T., Pregon, A., Pierrot, D., Poulter, B., Rehder, G., Resplandy, L., Robertson, E., Rodenbeck, C., Seferian, R., Schwinger, J., Smith, N., Tans, P. P., Tian, H., Tilbrook, B., Tubiello, F. N., van der Werf, G. R., Wiltshire, A. J., and Zaehle, S.: Global Carbon Budget 2019, Earth System Science Data, 11, 1783-1838, 10.5194/essd-11-1783-2019, 2019.

6. George, K., Ziska, L. H., Bunce, J. A., and Quebedeaux, B.: Elevated atmospheric CO₂ concentration and temperature across an urban-rural transect, Atmospheric Environment, 41, 7654-7665, 10.1016/j.atmosenv.2007.08.018, 2007.

7. Grimmond, C. S. B., King, T. S., Cropley, F. D., Nowak, D. J., and Souch, C.: Local-scale fluxes of carbon dioxide in urban environments: methodological challenges and results from Chicago, Environmental Pollution, 116, S243-S254, 10.1016/S0269-7491(01)00256-1, 2002.

8. Gross, B., Zheng, Z., Liu, S., Chen, X., Sela, A., Li, J., Li, D., and Havlin, S.: Spatio-temporal propagation of COVID-19 pandemics, <https://arxiv.org/abs/2003.08382>, 2020.

9. Han, P., Cai, Q., Oda, T., Zeng, N., Shan, Y., Lin, X., and Liu, D.: Assessing the recent impact of COVID-19 on carbon emissions from China using domestic economic data, The Science of the total environment, 750, 141688-141688, 10.1016/j.scitotenv.2020.141688, 2020.

10. Idso, C. D., Idso, S. B., and Balling, R. C.: The urban CO₂ dome of Phoenix, Arizona, Physical Geography, 19, 95-108, 10.1080/02723646.1998.10642642, 1998.

11. Idso, C. D., Idso, S. B., and Balling, R. C.: An intensive two-week study of an urban CO₂ dome in Phoenix, Arizona, USA, Atmospheric Environment, 35, 995-1000, 10.1016/S1352-2310(00)00412-X, 2001.

12. Idso, S. B., Idso, C. D., and Balling, R. C.: Seasonal and diurnal variations of near-surface atmospheric CO₂ concentration within a residential sector of the urban CO₂ dome of Phoenix, AZ, USA, Atmospheric Environment, 36, 1655-1660, 10.1016/S1352-2310(02)00159-0, 2002.

13. Khan, A., Schaefer, D., Tao, L., Miller, D. J., Sun, K., Zondlo, M. A., Harrison, W. A., Roscoe, B., and Lary, D. J.: Low Power Greenhouse Gas Sensors for Unmanned Aerial Vehicles, Remote Sensing, 4, 1355-1368, 10.3390/rs4051355, 2012.

14. Kutsch, W., Vermeulen, A., Karstens, U., 2020. Finding a hair in the swimming pool: the signal of changed fossil emissions in the atmosphere. <https://www.icos-cp.eu/event/917>.

15. Le Quere, C., Jackson, R. B., Jones, M. W., Smith, A. J. P., Abernethy, S., Andrew, R. M., De-Gol, A. J., Willis, D. R., Shan, Y., Canadell, J. G., Friedlingstein, P., Creutzig, F., and Peters, G. P.: Temporary reduction in daily global CO₂ emissions during the COVID-19 forced confinement, Nature Climate Change, 10.1038/s41558-020-0797-x, 2020.

LI-COR LI-7810 Brochure, access: 20Jun2020, 2019.

Liu, Z., Ciais, P., Deng, Z., Lei, R., Davis, S., Feng, S., Zheng, B., Cui, D., Dou, X., He, P., Zhu, B., Lu, C., Ke, P., Sun, T., Wang, Y., Yue, X., Wang, Y., Lei, Y., Zhou, H., Cai, Z., Wu, Y., Guo, R., Han, T., Xue, J., Boucher, O., Boucher, E., Chevallier, F., Wei, Y., Zhong, H., Kang, C., Zhang, N., Chen, B., Xi, F., Marie, F., Zhang, Q., Guan, D., Gong, P., Kammen, D., He, K., and Schellnhuber, H.: COVID-19 causes record decline in global CO₂ emissions, <https://arxiv.org/abs/2004.13614>, 2020.

16. Liu, Z., Ciais, P., Deng, Z., Lei, R., Davis, S. J., Feng, S., Zheng, B., Cui, D., Dou, X., Zhu, B., Guo, R., Ke, P., Sun, T., Lu, C., He, P., Wang, Y., Yue, X., Wang, Y., Lei, Y., Zhou, H., Cai, Z., Wu, Y., Guo, R., Han, T., Xue, J., Boucher, O., Boucher, E., Chevallier, F., Tanaka, K., Wei, Y., Zhong, H., Kang, C., Zhang, N., Chen, B., Xi, F., Liu, M., Brón, F., M., Lu, Y., Zhang, Q., Guan, D., Gong, P., Kammen, D. M., He, K., and Schellnhuber, H. J.: Near-real-time monitoring of global CO₂ emissions reveals the effects of the COVID-19 pandemic. Nat Commun. 2020 Oct 14;11(1):5172.

17. Martin, C. R., Zeng, N., Karion, A., Dickerson, R. R., Ren, X., Turpie, B. N., and Weber, K. J.: Evaluation and environmental correction of ambient CO₂ measurements from a low-cost NDIR sensor, Atmospheric Measurement Techniques, 10, 2383-2395, 10.5194/amt-10-2383-2017, 2017.

带格式的: 字体: (默认) Times New Roman

带格式的: 字体: (默认) Times New Roman

带格式的: 字体: (默认) Times New Roman

带格式的: 字体: (默认) Times New Roman

带格式的: 编号 + 级别: 1 + 编号样式: 1, 2, 3, ... + 起始编号: 1 + 对齐方式: 左侧 + 对齐位置: 0 厘米 + 缩进位置: 0.74 厘米

带格式的: 字体: (默认) Times New Roman

- 610 18. Mitchell, L. E., Lin, J. C., Bowling, D. R., Pataki, D. E., Strong, C., Schauer, A. J., Bares, R., Bush, S. E., Stephens, B. B., Mendoza, D., Mallia, D., Holland, L., Gurney, K. R., and Ehleringer, J. R.: Long-term urban carbon dioxide observations reveal spatial and temporal dynamics related to urban characteristics and growth, *Proceedings of the National Academy of Sciences of the United States of America*, 115, 2912-2917, 10.1073/pnas.1702393115, 2018.
19. Mueller, M., Graf, P., Meyer, J., Pentina, A., Brunner, D., Perez-Cruz, F., Hugglin, C., and Emmenegger, L.: Integration and calibration of non-dispersive infrared (NDIR) CO₂ low-cost sensors and their operation in a sensor network covering Switzerland, *Atmospheric Measurement Techniques*, 13, 3815-3834, 10.5194/amt-13-3815-2020, 2020.
20. Ott, L., Peters, G., Meyer, A., 2020. [Special virtual panel: Covid-19 and its impact on global carbon emissions.](https://carbon.nasa.gov/policy_speaker_28052020.html)
https://carbon.nasa.gov/policy_speaker_28052020.html.
- 615 21. Perez, I. A., Luisa Sanchez, M., Angeles Garcia, M., and de Torre, B.: CO₂ transport by urban plumes in the upper Spanish plateau, *Science of the Total Environment*, 407, 4934-4938, 10.1016/j.scitotenv.2009.05.037, 2009.
22. Picarro G2401 Analyzer Datasheet access: 20jul2020, 2017.
23. Picarro G2301 Analyzer Datasheet, access: 20Jun2020, 2019.
- 620 24. Rosenzweig, C., Solecki, W., Hammer, S. A., and Mehrotra, S.: Cities lead the way in climate-change action, *Nature*, 467, 909-911, 10.1038/467909a, 2010.
25. SenseAir: K30 products sheets, access: 20jul2020, 2019.
26. Shusterman, A. A., Teige, V. E., Turner, A. J., Newman, C., Kim, J., and Cohen, R. C.: The Berkeley Atmospheric CO₂ Observation Network: initial evaluation, *Atmospheric Chemistry and Physics*, 16, 13449-13463, 10.5194/acp-16-13449-2016, 2016.
- 625 27. Su, T., Li, Z., and Kahn, R.: [Relationships between the planetary boundary layer height and surface pollutants derived from lidar observations over China: regional pattern and influencing factors.](https://doi.org/10.5194/acp-18-15921-2018) *Atmos. Chem. Phys.*, 18, 15921-15935.
<https://doi.org/10.5194/acp-18-15921-2018>.
28. Sun, W., Deng, L., Wu, G., Wu, L., Han, P., Miao, Y., and Yao, B.: Atmospheric Monitoring of Methane in Beijing Using a Mobile Observatory, *Atmosphere*, 10, 10.3390/atmos10090554, 2019.
- 630 29. Sussmann, R., and Rettinger, M.: Can We Measure a COVID-19-Related Slowdown in Atmospheric CO₂ Growth? Sensitivity of Total Carbon Column Observations, *Remote Sensing*, 12, 10.3390/rs12152387, 2020.
30. Woodwell, G. M., Houghton, R. A., and Tempel, N. R.: ATMOSPHERIC CO₂ AT BROOKHAVEN, LONG-ISLAND, NEW-YORK - PATTERNS OF VARIATION UP TO 125 METERS, *Journal of Geophysical Research*, 78, 932-940, 10.1029/JC078i006p00932, 1973.
- 635 31. Zeng, N., Zhao, F., Collatz, G. J., Kalnay, E., Salawitch, R. J., West, T. O., and Guanter, L.: Agricultural Green Revolution as a driver of increasing atmospheric CO₂ seasonal amplitude, *Nature*, 515, 394-+, 10.1038/nature13893, 2014.
32. Analysis of road traffic operation in Beijing during COVID-19 in 2020, access: 31Aug2020, 2020.
- 640 33. Zhang, Z., Wong, M., and Lee, K.: Estimation of potential source regions of PM_{2.5} in Beijing using backward trajectories, *Atmospheric Pollution Research*, 6, 173-177, 10.5094/apr.2015.020, 2015.
34. Zheng, J., Dong, S., Hu, Y., and Li, Y.: Comparative analysis of the CO₂ emissions of expressway and arterial road traffic: A case in Beijing, *Plos One*, 15, 10.1371/journal.pone.0231536, 2020.
- 645

带格式的: 正文

带格式的: 编号 + 级别: 1 + 编号
样式: 1, 2, 3, ... + 起始编号:
1 + 对齐方式: 左侧 + 对齐位置:
0 厘米 + 缩进位置: 0.74 厘米

